ACS APPLIED MATERIALS & INTERFACES

Research Article

www.acsami.org

Multilayer Dual-Polymer-Coated Upconversion Nanoparticles for Multimodal Imaging and Serum-Enhanced Gene Delivery

Lu He,[†,‡] Liangzhu Feng,[§,‡] Liang Cheng,[§] Yumeng Liu,[†] Zhiwei Li,[§] Rui Peng,[§] Yonggang Li,*[,†] Liang Guo,*[,†] and Zhuang Liu*[,§]

[†]Department of Radiology, The First Affiliated Hospital of Soochow University, Suzhou, Jiangsu 215006, China

[§]Institute of Functional Nano & Soft Materials (FUNSOM) & Collaborative Innovation Center of Suzhou Nano Science and Technology, Soochow University, Suzhou, Jiangsu 215123, China

Supporting Information

ABSTRACT: Upconversion nanoparticles (UCNPs) have been widely explored for various bioapplications because of their unique optical properties, easy surface functionalization, and low cytotoxicity. Herein, we synthesize gadolinium (Gd^{3+})-doped UCNPs, which are modified first with poly(ethylene glycol) (PEG) and then with two layers of poly(ethylenimine) (PEI) via covalent conjugation and layer-by-layer assembly, respectively. Compared with UCNP-PEG@1×PEI with only one layer of PEI coating, the final complex, UCNP-PEG@2×PEI, with two PEI layers exhibits reduced cytotoxicity and enhanced gene transfection efficiency. It is interesting to find that while free PEI polymer is only effective in gene transfection in a serum-free medium and shows drastically reduced transfection ability if serum is added, UCNP-PEG@2×PEI is able to transfect cells in both serum-free and -containing media and, surprisingly, offers even higher gene transfection efficiency if serum is added. This is likely due to the formation of protein corona on the nanoparticle surface, which triggers the receptor-mediated endocytosis of our UCNP vectors. Considering the upconversion luminescence and magnetic resonance imaging contrasting ability of UCNPs, our novel nanovector could serve as a "trackable" gene-delivery carrier promising for theranostic applications.

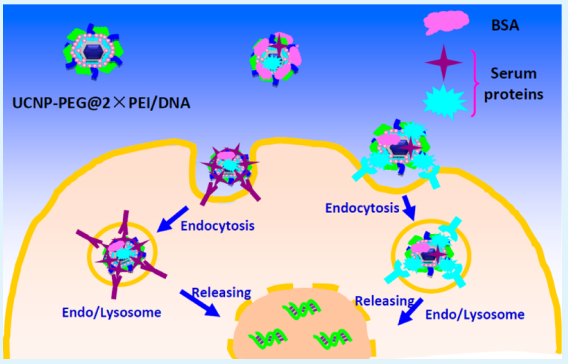

KEYWORDS: *upconversion nanoparticles, gene delivery, surface-coating effect, serum effect*

1. INTRODUCTION

Lanthanide-doped rare-earth upconversion nanoparticles (UCNPs), which are able to emit high-energy photons under excitation by near-infrared (NIR) light, have found potential applications in many different fields including nanobiomedicine.[1−5] Upconversion luminescence (UCL) imaging based on UCNPs shows a number of unique advantages over traditional fluorescence imaging, such as enhanced tissue penetration, better photostability, and a essentially eliminated autofluorescence background that allows ultrasensitive in vivo detection.[1,6−9] In recent years, many research groups have explored the potential use of UCNPs for disease diagnosis and therapy.[7,10−13] Biosensing with UCNP probes has been widely explored to enable the detection of various biological species via different mechanisms.[14−17] In the area of biomedical imaging, UCNPs not only have been extensively applied in UCL optical imaging of various biological systems but also could be engineered to acquire multiple functionalities to serve as novel imaging probes in multimodal imaging.[17−25] Moreover, UCNPs recently have also shown great promise in cancer therapies including their use as drug-delivery carriers to enable NIR-induced photodynamic therapy and to realize imaging-guided cancer theranostics.[7,10,12,15,23,26−30]

Gene therapy can be defined as the use of gene materials, such as DNA or small interfering RNA molecules, to treat or prevent diseases.[31−33] Despite the high efficiency of using viral vectors in gene delivery, nonviral vectors have their advantages in terms of simple use, ease of production, lower concerns in terms of biosafety, and the lack of specific immune response. In recent years, many nanoparticle-based gene vectors have been developed by many different research teams. Many of those nanoparticles, such as fluorescent quantum dots, magnetic nanoparticles, and gold nanoparticles, not only could be engineered to act as effective gene-delivery vectors but also are useful imaging probes to allow real-time tracking for imaging-guided gene therapy.[34−40] Recently, there have been two groups reporting the use of UCNPs for NIR-triggered gene delivery.[41,42] In their design, UCNPs, which serve as gene carriers as well as imaging probes, could also allow NIR-induced release of cargo DNA or RNA molecules for light-controllable gene delivery. However, further careful studies are still needed to understand the surface-coating effect of UCNP-

Received: August 22, 2013
Accepted: September 26, 2013
Published: September 26, 2013

based gene carriers and optimize their performance in various physiological conditions, especially in the presence of serum proteins, to allow their potential use as theranostic platforms for in vivo gene therapy.

Therefore, in this study, we synthesize Gd^{3+}-containing UCNPs modified with dual-type polymers, poly(ethylene glycol) (PEG) and two layers of poly(ethylenimine) (PEI), and use the obtained UCNP-PEG@2×PEI complex as an effective gene-delivery vector for the transfection of plasmid DNA (pDNA) encoding enhanced green fluorescent protein (Figure 1a). Compared with free PEI and UCNP-PEG@1×PEI

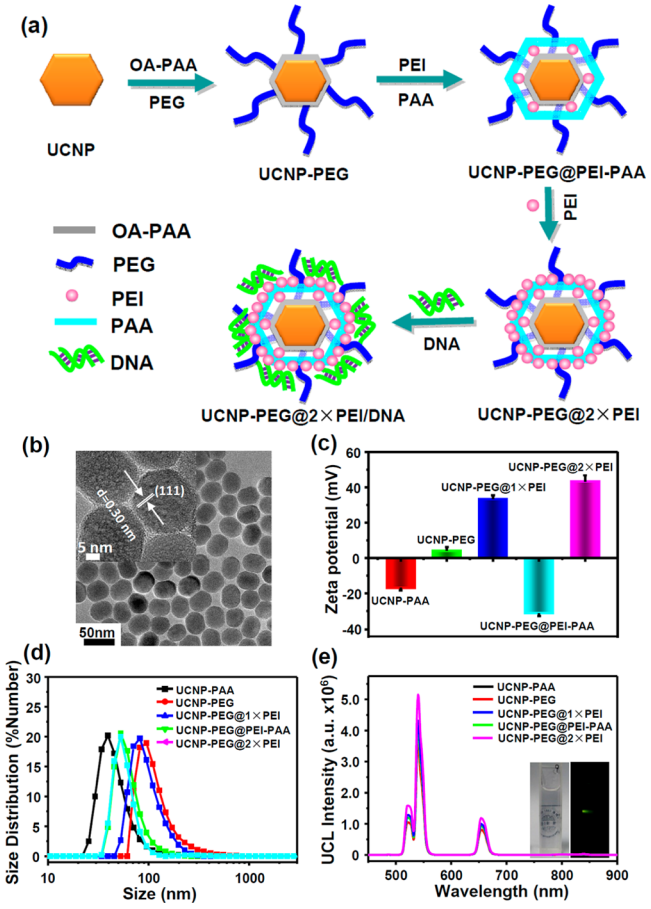

Figure 1. Preparation of UCNP-based gene vector. (a) Schematic illustration showing the synthesis of UCNP-PEG@2×PEI and the subsequent pDNA binding. (b) TEM images of as-made UCNPs. The inset shows the HRTEM image of UCNPs. (c) ζ potentials (c) and DLS data (d) of UCNPs after various layers of polymer coatings measured in water. (e) UCL spectra of UCNPs after various layers of polymer coatings recorded at the same UCNP concentration. The inset shows a photograph of the UCNP-PEG@2×PEI sample under ambient light (left) or exposed to a 980 nm laser (right).

with one PEI layer, UCNP-PEG@2×PEI shows significantly reduced cytotoxicity. Regarding gene transfection under serum-free conditions, UCNP-PEG@2×PEI offers much better efficiency than UCNP-PEG@1×PEI but is slightly less effective than free PEI. Interestingly, when serum is added during transfection, PEI becomes ineffective in gene transfection, while in marked contrast, UCNP-PEG@2×PEI shows remarkably enhanced transfection efficiency. We hypothesize that this phenomenon is likely due to enhanced receptor-mediated endocytosis via the binding of serum proteins, which form a corona on the nanoparticle surface with the cell membrane receptors, which recognize certain serum proteins. Thus, our UCNP-based gene-delivery system developed here may be a promising imaging-trackable gene vector that works well in the presence of serum proteins.

2. MATERIALS AND EXPERIMENTS

2.1. Materials. Branched poly(ethylenimine) (PEI) with a molecular weight (MW) of 25 kDa, poly(acrylic acid) (PAA) with a MW of 100 kDa, *N*-[3-(dimethylamino)propyl-*N*′-ethylcarbodiimide] hydrochloride (EDC), 3-(4,5-dimethylthiazol-2-yl)-2,5-diphenyltetrazolium bromide (MTT), and propidium iodide (PI) were purchased from Sigma-Aldrich (USA). Six-armed amine-terminated poly(ethylene glycol) (PEG) with a MW of 10 kDa was purchased from Sunbio (South Korea). Agarose, 4′,6-diamidino-2-phenylindole (DAPI), and fetal bovine serum (FBS) were purchased from Invitrogen (USA). Dulbecco's modified Eagle's medium (DMEM) and RPMI-1640 were purchased from Thermo Scientific (USA). Albumin bovine V (M_r = 68000) was purchased from Solarbio (China). Transferrin (Holo) was purchased from MP Biomedicals (France). Enhanced green fluorescent protein (EGFP) plasmid was prepared according to our previous modified method.[43]

Monodispersed hexagonal $NaGdF_4$-based UCNPs (Gd:Yb:Er = 78:20:2) were synthesized according to literature protocols with slight modifications.[44−47] The as-prepared UCNPs were modified with octylamine (OA)−PAA copolymer, which was synthesized following a literature protocol.[48] The obtained UCNP-PAA was further conjugated with PEG by mixing UCNPs (1 mg mL^{-1}) with six-armed PEG (1 mg mL^{-1}) under sonication for 5 min and then adding EDC (2 mg mL^{-1}) to induce amide formation. After being stirred at room temperature for 30 min, the mixture was added with PEI (50 mg mL^{-1}) and EDC (2 mg mL^{-1}) following another 5 min of sonication. After stirring at room temperature for 8 h, the mixture was purified by centrifugation (14800 rpm, 5 min) and washed three times with deionized (DI) water. As-prepared UCNP-PEG@1×PEI (1 mg mL^{-1}) was further coated with PAA (10 mg mL^{-1}) in the presence of EDC (2 mg mL^{-1}) and then washed with DI water three to five times to remove excess PAA after being stirred at room temperature for 8 h. Afterward, the obtained UCNP-PEG@PEI-PAA (1 mg mL^{-1}) was further conjugated with PEI (10 mg mL^{-1}) in the presence of EDC (2 mg mL^{-1}). After being stirred at room temperature for another 8 h, the mixture was purified by centrifugation, forming UCNP-PEG@2×PEI. The obtained UCNP-PAA, UCNP-PEG, UCNP-PEG@1×PEI, UCNP-PEG@PEI-PAA, and UCNP-PEG@2×PEI were stored at 4 °C for the following experiments.

Transmission electron microscopy (TEM) images of those nanoparticles were taken by a Tecnai G2F20 transmission electron microscope (FEI Company). The concentrations of UCNP-PEG@1×PEI and UCNP-PEG@2×PEI were qualified by recording the concentrations of Gd^{3+} using inductively coupled plasma mass spectrometry (ICP-MS). Elemental analysis data, ζ potentials, size distributions, and UCL spectra of UCNP-PAA, UCNP-PEG, UCNP-PEG@1×PEI, UCNP-PEG@PEI-PAA, and UCNP-PEG@2×PEI were obtained by an elemental analyzer (EA1110 CHNO-S, Carlo Erba), a Nano-ZS90 nanoparticle analyzer (Malvern Instruments Ltd.), and a FluoroMax-4 luminescent spectrometer (Horiba JobinYvon SAS), respectively.

2.2. Cell Culture. Human cervical cancer HeLa cells, human hepatoma HepG2 cells, and human embryonic kidney 293T cells were cultured in DMEM containing 10% FBS and 1% penicillin/streptomycin at 37 °C in a humidified 5% CO_2-containing atmosphere. Human breast cancer MCF-7 cells were cultured in a RPMI-1640 cell medium containing 10% FBS and 1% penicillin/streptomycin at 37 °C in a humidified 5% CO_2-containing atmosphere.

2.3. In Vitro Cytotoxicity Assay. The cytotoxicities of UCNP-PEG@1×PEI, UCNP-PEG@2×PEI, and a bare PEI polymer were evaluated on HeLa cells by the standard MTT assay. In brief, HeLa cells were seeded in 96-well plates at a density of 1×10^4 cells $well^{-1}$ and incubated at 37 °C for 24 h before the experiment. Then, a series

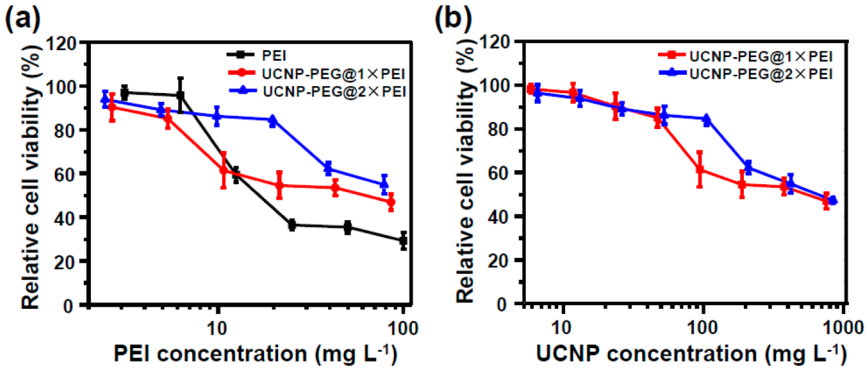

Figure 2. In vitro cytotoxicity assay. Relative cell viability data of HeLa cells after being incubated with a series of concentrations of free PEI, UCNP-PEG@1×PEI, and UCNP-PEG@2×PEI for 24 h. Data are presented based on either PEI (a) or UCNP (b) concentrations. Error bars were based on triplicate samples.

of concentrations of UCNP-PEG@1×PEI, UCNP-PEG@2×PEI, and a bare PEI polymer were added into the cell cultures. After 24 h of incubation, 25 μL of a MTT solution in phosphate-buffered saline (PBS; 5 mg mL^{-1}) was added to each well and incubated for an additional 4 h. The cell culture was discarded afterward with 150 μL of dimethyl sulfoxide added into each well. We then incubated the plate at 37 °C for 5 min and shocked it for another 10 min at room temperature to allow complete dissolution of formazan. Finally, the absorbance at 570 nm of each well was measured by a microplate reader (Bio-Rad model 680) to determine the relative cell viability.

2.4. Magnetic Properties of UCNP-PEG@2×PEI and Gd-DTPA. UCNP-PEG@2×PEI solutions with concentrations ranging from 0 to 1.22 mM of gadolinium and Gd-DTPA solutions with concentrations ranging from 3.88 to 11.9 mM of gadolinium were scanned under a magnetic resonance imaging (MRI) scanner (Bruker Biospin Corp., Billerica, MA) at room temperature. After the T1-weighted MRI images were acquired, the signal intensity was measured within a manually drawn region-of-interest for each sample. R1 values (R1 = 1/T1) were calculated from T1 values at different gadolinium concentrations.

2.5. Multimodal in Vitro Imaging of HeLa Cells. MRI images of cells were performed using a series of UCNP-PEG@2×PEI solutions with different concentrations to incubate with HeLa cells for 4 h. The concentrations of UCNP-PEG@2×PEI solutions ranged from 4.34 to 69.4 μg mL^{-1}.

Fluorescence images of cells were taken using a modified Leica laser scanning confocal microscope (Leica TCS SPII, Germany) with a continuous-wave (CW) NIR laser (Connet Fiber Optics, China) at 980 nm as an additional excitation source. HeLa cells were seeded into 24-well plates at a density of about 1 × 10^5 cells well^{-1} 24 h before UCNP-PEG@2×PEI solutions were added. The added concentrations of UCNP-PEG@2×PEI were equivalent to those added in MRI. After being incubated with UCNP-PEG@2×PEI for 4 h, the cells were washed with PBS sufficiently, fixed with 4% formaldehyde, stained with DAPI, and then imaged by the confocal microscope.

2.6. Preparation of UCNP-PEI/EGFP Plasmid Complexes and Gel Electrophoresis Assay. Appropriate amounts of a bare PEI polymer, UCNP-PEG@1×PEI, and UCNP-PEG@2×PEI were mixed with 1 μg of EGFP plasmid DNA in 30 μL of DI water at N/P ratios of 1, 2, 5, 10, and 20. For the mixtures of UCNP-PAA and pDNA, the amounts of added UCNPs were equivalent to the amounts of UCNPs in UCNP-PEG@2×PEI/pDNA at N/P ratios of 10 and 20. After incubation for 30 min at room temperature, the samples were analyzed by 0.8% agarose gel electrophoresis using a triacetate−ethylenediaminetetraacetic acid buffer solution as the running buffer.

2.7. In Vitro EGFP Plasmid Transfection. HeLa cells were seeded in 24-well plates at a density of about 1 × 10^5 cells well^{-1} 24 h before transfection. We diluted 1 μg of EGFP plasmid in 100 μL of serum-free DMEM and also diluted appropriate amounts of a bare PEI polymer, UCNP-PEG@1×PEI, and UCNP-PEG@2×PEI in 100 μL of serum-free DMEM. After 10 s of vortexing, the two solutions were mixed and incubated for 30 min at room temperature before being added into cells. All cells were washed two times with a serum-free medium right before the addition of transfection complexes. After 4 h of incubation, the transfection complexes were removed and cells were washed two times with a serum-free medium before the addition of 1 mL of formal DMEM containing 10% FBS. An additional 44 h of incubation was needed for efficient EGFP expression. We also assessed the transfection efficiencies of UCNP-PEG@2×PEI and a bare PEI polymer in the presence of serum. We chose the N/P ratio of 10 as the optimal ratio, and the added amounts of transfection complexes were equivalent to those added under serum-free conditions.

Both confocal fluorescence microscopy and flow cytometry were employed to determine the EGFP transfection efficiencies after various treatments. An excitation wavelength of 488 nm and an emission band between 500 and 600 nm were chosen for the fluorescence imaging of EGFP plasmid transfected cells. All images were taken under the same parameter setting. Cells were quantitatively analyzed by a BD flow cytometer (BD Bioscience, Bedford, MA), after they were briefly incubated in 300 μL of PBS containing a 1 μg mL^{-1} PI solution with the purpose of staining the dead cells.

3. RESULTS AND DISCUSSION

In this work, we used $NaGdF_4$-based UCNPs (Gd:Yb:Er = 78:20:2) as nanovectors for multimodal imaging and gene delivery. A TEM image revealed that the synthesized UCNPs were monodispersed hexagonal nanocrystals with an average diameter of ∼30 nm (Figure 1b). A high-resolution TEM (HRTEM) image showed the lattice fringes with a d spacing of 0.30 nm, in good agreement with the lattice spacing of the (111) planes of hexagonal $NaGdF_4$ (JCPD 27-0697; Figures 1b and S1 in the Supporting Information, SI). UCNPs, after first being modified with an OA−PAA copolymer, were conjugated with PEG and two layers of PEI. The ζ potentials of UCNP-PAA and UCNP-PEG were measured as −16.9 and +4.07 mV, respectively. UCNP-PEG@1×PEI with positively charged PEI coating showed a further increased ζ potential as +33.7 mV, which decreased to −31.25 mV after PAA coating, and then jumped back to +43.25 mV after the second layer of PEI coating (Figure 1c). Interestingly, dynamic light scattering (DLS) data revealed the obviously reduced hydrodynamic sizes of those nanoparticles when the first and second layers of PEI coating were introduced, suggesting that the positively charged PEI coating would make the polymer shell on UCNPs more condensed (Figure 1d). The final product, UCNP-PEG@2×PEI, exhibited good dispersibility without obvious agglomeration in various physiological solutions including saline (0.9% NaCl), PBS, serum, and a cell culture medium (Figure S2 in the SI).

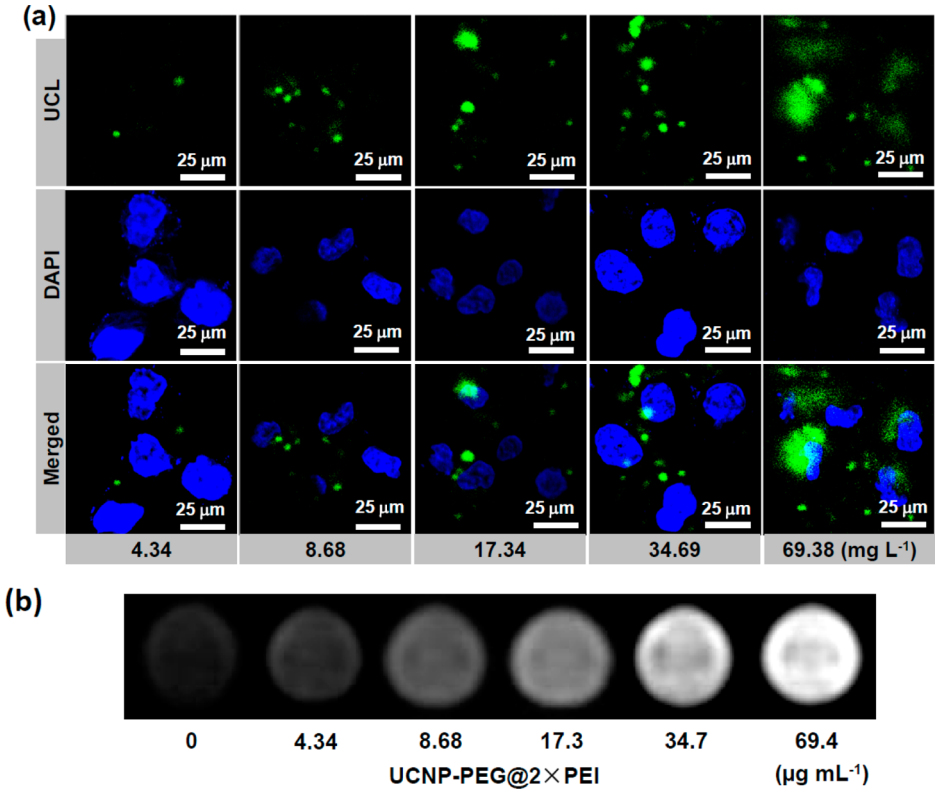

Figure 3. Multimodal in vitro cell imaging. HeLa cells were incubated with UCNP-PEG@2×PEI for 4 h at various concentrations prior to imaging. (a) Confocal UCL/fluorescence images of cells. Green and blue colors represent UCL signals of UCNPs and DAPI stained cell nuclei, respectively. (b) T1-weighted MRI images of UCNP-incubated HeLa cells. The cells were suspended in 1% agarose gel for MRI.

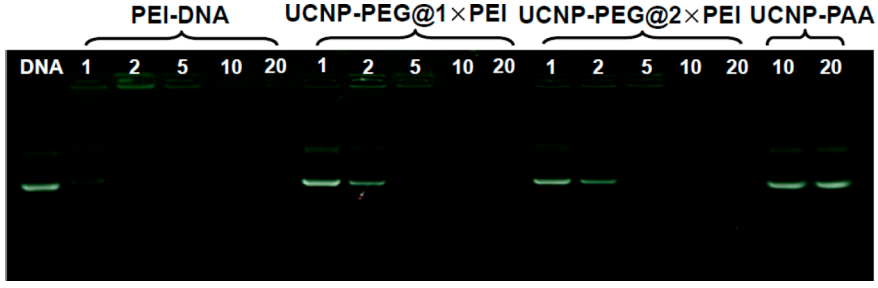

Figure 4. Gel retardation assay. Agarose gel electrophoresis of bare EGFP pDNA and pDNA mixed with free PEI, UCNP-PEG@1×PEI, and UCNP-PEG@2×PEI, as well as PAA-modified UCNPs at different N/P ratios. Each sample was incubated at room temperature for 30 min before electrophoresis. The amounts of UCNPs used in the UCNP-PAA/pDNA samples were identical with the UCNP quantities in the UCNP-PEG@2×PEI/pDNA samples at N/P ratios of 10 and 20.

The UCL spectra of UCNP-PAA, UCNP-PEG, UCNP-PEG@1×PEI, UCNP-PEG@PEI-PAA, and UCNP-PEG@2×PEI displayed emission peaks around 540 and 660 nm, with similar emission intensities for all of the samples at the same UCNP concentration (Figure 1e). After 2×PEI was coated on the surface of UCNP-PEG, the UCL intensity was slightly decreased to 80%. The nitrogen contents of UCNP-PEG@1×PEI and UCNP-PEG@2×PEI were measured by an elemental analyzer as 5.0% and 15.7%, respectively (Table S1 in the SI). Hence, the corresponding weight ratios of UCNP:PEI in UCNP-PEG@1×PEI and UCNP-PEG@2×PEI respectively were 17.6:1 and 5.36:1.

Gadolinium-containing UCNPs have been widely exploited as multimodal imaging probes for UCL imaging and T1-weighted MRI.[19,20] We next studied the magnetic properties of those gadolinium-based UCNPs. A series of UCNP-PEG@2×PEI solutions and Gd-DTPA solutions with different gadolinium molar concentrations were recorded by a 3.0 T MRI scanner. T1-weighted MRI images of UCNP-PEG@2×PEI and Gd-DTPA solutions revealed a concentration-dependent brightening effect (Figure S3a,b in the SI). A good linear relationship was observed, with the R1 value of UCNP-PEG@2×PEI determined as 2.37 mM^{-1} s^{-1}, which was higher than that of Gd-DTPA (Figure S3c,d in the SI).

To evaluate the biocompatibility of UCNP-PEG@1×PEI and UCNP-PEG@2×PEI, the relative viabilities of HeLa cells after being incubated with a bare PEI polymer, UCNP-PEG@1×PEI, and UCNP-PEG@2×PEI for 24 h were determined via the standard MTT assay (Figure 2). Our results showed that after 24 h of incubation, UCNP-PEG@2×PEI showed the lowest cytotoxicity at the same PEI concentration, in comparison to a bare PEI polymer and UCNP-PEG@1×PEI with one layer of PEI coating (Figure 2a). Interestingly, even based on the UCNP concentration, UCNP-PEG@2×PEI with

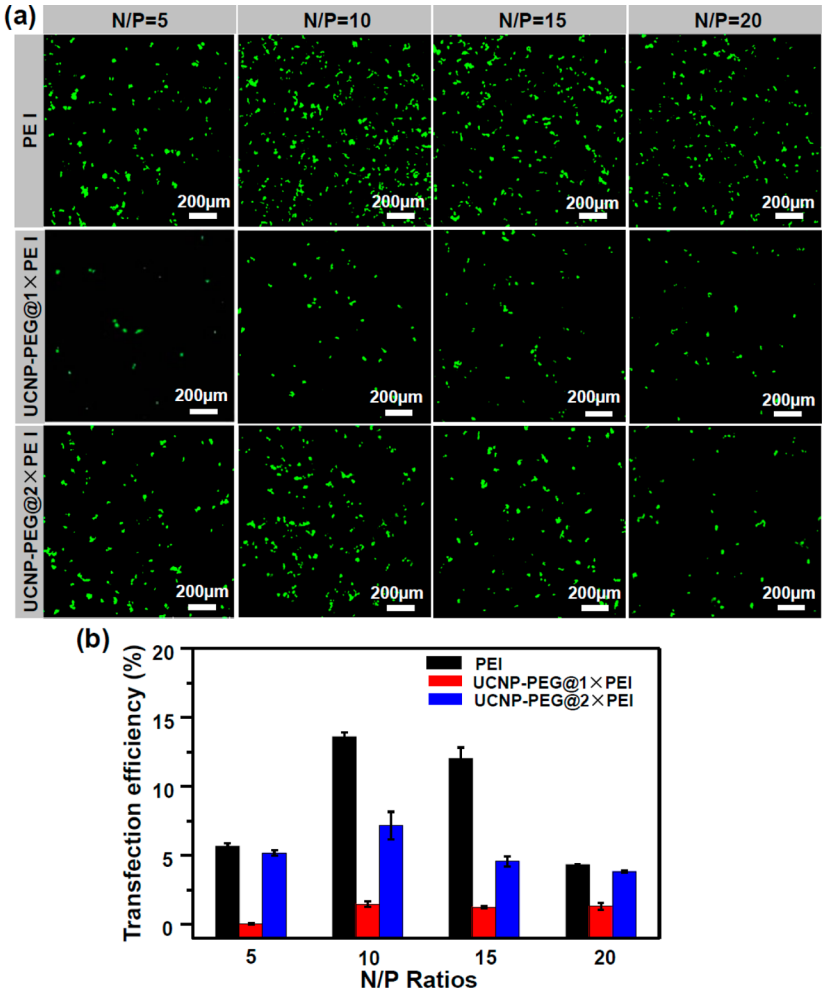

Figure 5. Gene transfection under serum-free conditions. (a) Confocal fluorescence images of EGFP-transfected HeLa cells measured 48 h after the initiation of transfection using free PEI, UCNP-PEG@1×PEI, and UCNP-PEG@2×PEI under serum-free conditions at varying N/P ratios from 5 to 20. (b) EGFP transfection efficiencies by different vectors under varying N/P ratios as determined by flow cytometry.

more PEI per nanoparticle was still obviously less toxic than UCNP-PEG@1×PEI (Figure 2b). Previous studies have revealed that cationic polymers such as PEI would induce cytotoxicity by binding with plasma membranes, while after the polymers were coated on certain nanoparticles, their cytotoxicities could be reduced because of the resulting lower density of cationic residues interacting with the cells.[49,50] The reduced toxicity of UCNP-PEG@2×PEI was likely attributed to a similar mechanism. Thus, the UCNP-PEG@2×PEI complex appeared to be much safer than a bare PEI polymer and UCNP-PEG@1×PEI.

We next demonstrated the capability of using UCNP-PEG@2×PEI in multimodal imaging. HeLa cells were incubated with various concentrations of UCNP-PEG@2×PEI for 4 h and then imaged by either UCL optical imaging or MRI. The UCL signals enhanced along with the increased concentrations of UCNP-PEG@2×PEI during incubation (Figure 3a). Meanwhile, T1-weighted MRI images of those cells also showed a concentration-dependent brightening effect (Figure 3b). Therefore, our UCNPs could serve as a dual-modal nanoprobe for both UCL imaging and MRI.

To study the pDNA binding ability of our nanoparticles, we next mixed a bare PEI polymer, UCNP-PEG@1×PEI, UCNP-PEG@2×PEI, and UCNP-PAA with EGFP plasmid at different N/P ratios and carried out a gel electrophoresis assay (Figure 4). When UCNP-PEG@1×PEI and UCNP-PEG@2×PEI were both mixed with EGFP plasmid at a N/P ratio above 5, significant retardation of plasmid moving in gel electrophoresis was observed. In contrast, UCNP-PAA without PEI conjugation could not retard EGFP plasmid.

We then tested the gene transfection efficiencies of a bare PEI polymer, UCNP-PEG@1×PEI, and UCNP-PEG@2×PEI for EGFP plasmid transfection on HeLa cells under the standard serum-free conditions at different N/P ratios. Judging from the number of bright cells in confocal fluorescent images, without the existence of serum, UCNP-PEG@1×PEI and UCNP-PEG@2×PEI were able to transfect HeLa cells with EGFP plasmid at N/P ratios from 5 to 20, while the transfection efficiencies of UCNP-PEG@1×PEI were lower than that of UCNP-PEG@2×PEI at the same N/P ratio. A bare PEI polymer displayed superior transfection efficiency at N/P ratios of 10 and 15 but showed severe cytotoxicity at even higher N/P ratios (Figure 5a). Apart from being qualitatively analyzed by confocal laser scanning microscopy (CLSM), the transfection efficiencies of UCNP-PEG@1×PEI, UCNP-PEG@2×PEI, and a bare PEI polymer were quantitatively analyzed by flow cytometry, and the results were consistent with those detected by CLSM (Figure 5b).

Although serum-free conditions are commonly used during transfection when PEI and many other commercial transfection

agents (e.g. lipofectamine) are employed, for in vivo applications the transfection ability of an effective gene vector should not be affected by the existence of serum proteins. Next, we wondered how the presence of serum would effect EGFP transfection by the UCNP-based gene vectors developed in this work. Compared to the serum-free conditions, it is worth noting that the transfection efficiencies of UCNP-PEG@2×PEI in serum-containing conditions improved. At a N/P ratio of 10, the transfection efficiency of UCNP-PEG@2×PEI increased from 7.2% in a serum-free medium to 43.8% in 10% FBS-containing conditions. In cell cultures containing 20% and 30% FBS, the EGFP transfection efficiencies were still very high, with 48.6% and 38.0% of the cells successfully transfected with EGFP. In marked contrast, along with the increasing percentages of FBS, the transfection efficiencies of a bare PEI polymer dropped sharply (Figure 6), consistent with previous literature reports.[51]

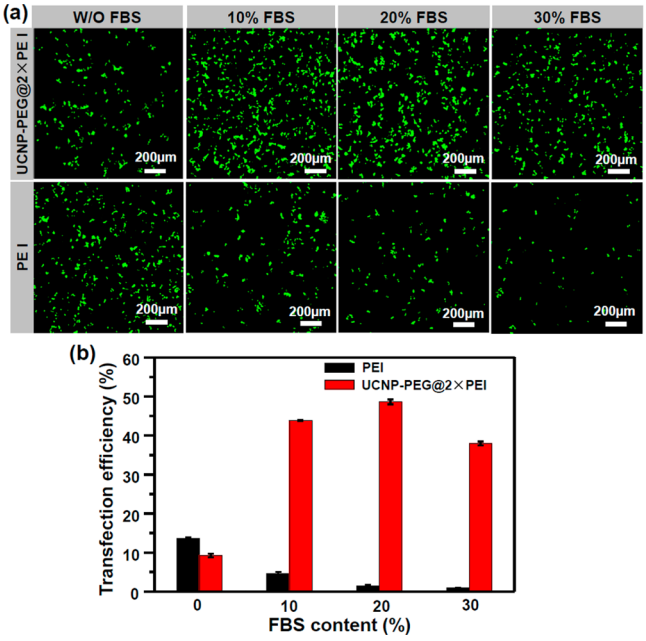

Figure 6. Serum effect in gene transfection. (a) Confocal fluorescence images of HeLa cells transfected with EGFP plasmid by using free PEI or UCNP-PEG@2×PEI at a N/P ratio of 10 in the presence of various concentrations of FBS. Those images were taken 48 h after the initiation of transfection. (b) FBS-dependent EGFP transfection efficiencies using a bare PEI polymer or UCNP-PEG@2×PEI as determined by flow cytometry. The presence of FBS would inhibit the gene transfection activity of bare PEI but would greatly promote transfection with UCNP-PEG@2×PEI.

The phenomenon that UCNP-PEG@2×PEI showed dramatically increased transfection efficiency in the presence of FBS was also confirmed in some other cell lines (Figure 7a). We chose three other cell lines including 293T, HepG2, and MCF-7 cells, in our experiments, and conducted EGFP plasmid transfection using UCNP-PEG@2×PEI in cell cultures containing 0%, 10%, 20%, and 30% of FBS. In addition to HeLa cells, all of the other three types of cells showed serum-promoted gene transfection behaviors in the presence of FBS when UCNP-PEG@2×PEI was used as the gene vector, although the enhancement was less obvious for 293T and MCF-7 cells.

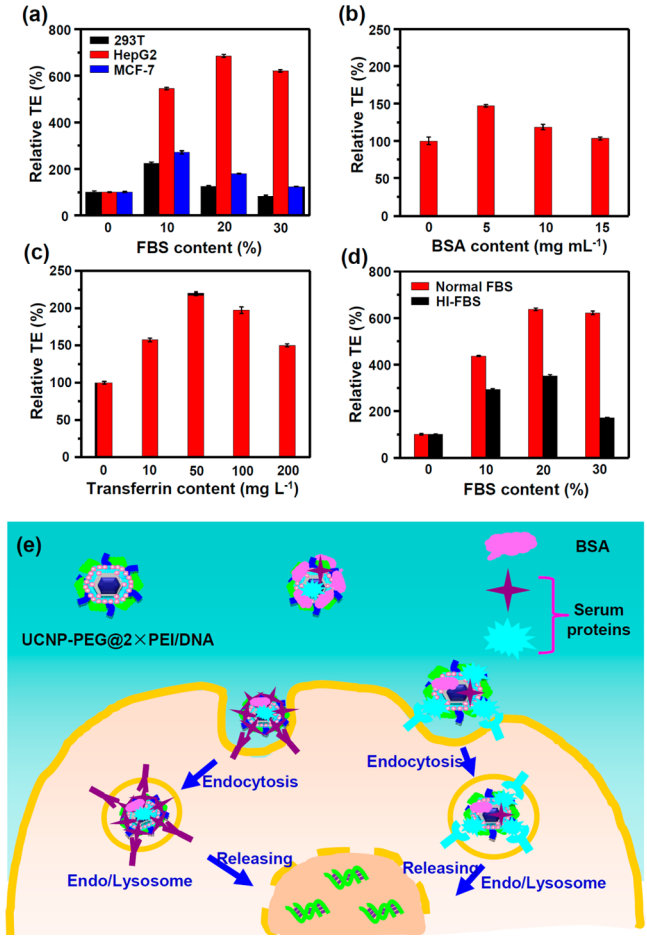

Figure 7. Understanding the serum-dependent gene transfection behaviors of a UCNP-based gene vector. The relative transfection efficiencies (TEs) were recorded by flow cytometry measurement. (a) Relative EGFP gene transfection efficiencies of UCNP-PEG@2×PEI transfected 293T, HepG2, and MCF-7 cells in the presence of various FBS contents. (b and c) Relative transfection efficiencies of HeLa cells by UCNP-PEG@2×PEI in a serum-free cell medium supplemented with different BSA contents (b) or transferrin concentrations (c). (d) Relative transfection efficiencies of HeLa cells by UCNP-PEG@2×PEI in cell cultures containing 10% normal serum or 10% HI serum. The above experiments were conducted at the optimal N/P ratio of 10. (e) Scheme showing our proposed mechanism of serum-enhanced gene transfection with our UCNP vectors.

Although PEI has excellent pDNA binding ability, it was found that the formed PEI/pDNA complexes were not stable in the presence of serum proteins, showing rapidly increased hydrodynamic diameters once serum was added (Figure S4 in the SI), owing to the nonspecific adsorption of proteins on the positively charged PEI/pDNA complexes that resulted in their agglomeration.[52,53] On the contrary, the UCNP-PEG@2×PEI/pDNA complexes with the help of PEG showed markedly improved stability in the presence of serum without showing significant serum-induced aggregation (Figure S4 in the SI). Such phenomena explained why the gene transfection with PEI, but not UCNP-PEG@2×PEI, was negatively effected by serum. However, the mechanism of serum-enhanced EGFP transfection by UCNP-PEG@2×PEI remained unknown.

We thus wondered why the existence of serum would promote the transfection efficiency of UCNP-PEG@2×PEI. Through tracking of the intrinsic UCL emissions of UCNPs,

confocal UCL images of HeLa cells incubated with UCNP-PEG@2×PEI were recorded by a confocal microscope (Figure S5 in the SI). Consistent with the transfection results, the cellular uptake of UCNPs also obviously increased upon the addition of FBS. Serum contains a wide range of proteins, with albumin as the major component. The enhanced gene transfection of UCNP-PEG@2×PEI is thus likely due to the formation of protein corona on the nanoparticle surface, which promotes the cellular uptake of those nanoparticles.[54,55]

Because bovine serum albumin (BSA) is the most abundant component of FBS (1.33−1.90%), we tested the EGFP transfection with HeLa cells using UCNP-PEG@2×PEI in a serum-free cell culture but with BSA added. On the basis of flow cytometry data to determine the percentages of EGFP-expressing cells, it was found that the addition of BSA only slightly increased the transfection efficiency (Figure 7b). Therefore, although BSA is the major component of FBS, its role in promoting the cellular uptake of nanoparticles may not be the most important.

Transferrin is another type of protein existing inside serum with a concentration of 1.2−1.8 mg mL^{-1}.[56] Many types of cells, including HeLa and HepG2 cells, overexpress transferrin receptor (TfR) on their membrane to recognize transferrin.[57−60] To see if transferrin would have any effect on gene transfection with UCNP-PEG@2×PEI, we carried out EGFP transfection with UCNP-PEG@2×PEI on HeLa cells in a serum-free medium but with the addition of transferrin at different concentrations ranging from 10 to 200 μg mL^{-1}. Interestingly, the existence of transferrin did offer significant enhancement regarding the EGFP transfection with UCNP-PEG@2×PEI, by over 2-fold when 50 μg mL^{-1} of transferrin was added (Figure 7c). However, the enhancement factor achieved here was still not as high as that in serum-containing conditions, indicating that besides transferrin there could be some other substances in serum that helped UCNP-PEG@2×PEI in the process of gene delivery.

It has been found that many types of nanoparticles could induce complement activation in serum to varied extents.[61,62] Heat inactivation (HI) by incubating serum at high temperature (e.g., 56 °C) for a certain period (e.g., 30 min) is a procedure commonly applied in the cell culture to destroy the complement activity in the serum. We then tested the EGFP transfection by UCNP-PEG@2×PEI on HeLa cells with cell cultures supplemented with either non-HI normal serum or HI serum. Compared with the gene transfection efficiencies of UCNP-PEG@2×PEI in the presence of normal serum, those obtained in cell culture with HI serum were dramatically lower (Figure 7d). Thus, it is likely that a range of different proteins, possibly including those involved in a complementary activation system, could contribute to the enhanced cellular uptake of nanoparticles and subsequently the increased gene transfection efficiency when UCNP-PEG@2×PEI is used as the gene vector (Figure 7e).

4. CONCLUSIONS

In summary, we design a new type of surface-coating strategy to functionalize UCNPs and render them excellent gene transfection ability. In such a design, UCNPs, which could serve as imaging probes for dual-modal optical imaging and MRI, are first conjugated with PEG to acquire physiological stability and then coated with one or two layers of PEI polymers to obtain gene loading ability. It is found that two layers of PEI coatings offer nanoparticle reduced cytoxicity and enhanced gene transfection ability compared to those with only one PEI layer. In comparison with PEI, our UCNP-PEG@2×PEI complex shows much lower toxicity and slightly lower transfection ability in the absence of serum. Notably, the existence of serum, which largely inhibits the transfection activity of PEI, would greatly promote the EGFP transfection with UCNP-PEG@2×PEI. This is possibly owing to the formation of protein corona on the particle surface, which, on the one hand, would not reduce the stability of nanoparticles because of the existence of PEG and, on the other hand, could induce the receptor-mediated endocytosis to promote cellular uptake of nanoparticles and thus the gene transfection. Our work not only highlights the promise of UCNP-PEG@2×PEI as a novel imaging-trackable nanovector for safe and efficient gene delivery in vitro and potentially in vivo but also suggests that well-engineered surface chemistry is critical in the development of other types of nanoparticle-based gene-delivery vectors.

■ ASSOCIATED CONTENT

Supporting Information

XRD data, results of stability tests, MRI data of UCNPs, nitrogen and carbon contents of UCNP-PEG@2×PEI nanoparticles, DLS data of nanoparticles in cell cultures, and confocal UCL/fluorescence images of HeLa cells incubated with UCNP-PEG@2×PEI. This material is available free of charge via the Internet at http://pubs.acs.org.

■ AUTHOR INFORMATION

Corresponding Authors

*E-mail: liyonggang224@163.com.
*E-mail: ilguoliang@sohu.com.
*E-mail: zliu@suda.edu.cn.

Author Contributions

‡These two authors contributed equally to this work.

Notes

The authors declare no competing financial interest.

■ ACKNOWLEDGMENTS

This work was partially supported by the National Basic Research Program (973 Program) of China (Grants 2012CB932600 and 2011CB911002), the National Natural Science Foundation of China (Grants 81171394, 81171392, 51222203, 51132006, 51002100, and 51302180), the Natural Science Fund of Jiangsu Province (Grants BK2011307 and BK20130305), the Natural Science Fund for Colleges and Universities in Jiangsu Province (Grant 09KJB320016), the Postdoctoral Science Foundation of China (Grant 2013M531400) and the postdoctoral research program of Jiangsu Province (Grant 1202044C).

■ REFERENCES

(1) Wang, L.; Yan, R.; Huo, Z.; Wang, L.; Zeng, J.; Bao, J.; Wang, X.; Peng, Q.; Li, Y. *Angew. Chem., Int. Ed.* **2005**, *44*, 6054−6057.
(2) Mai, H.-X.; Zhang, Y.-W.; Si, R.; Yan, Z.-G.; Sun, L.-d.; You, L.-P.; Yan, C.-H. *J. Am. Chem. Soc.* **2006**, *128*, 6426−6436.
(3) Jin, J.; Gu, Y.-J.; Man, C. W.-Y.; Cheng, J.; Xu, Z.; Zhang, Y.; Wang, H.; Lee, V. H.-Y.; Cheng, S. H.; Wong, W.-T. *ACS Nano* **2011**, *5*, 7838−7847.
(4) Chatterjee, D. K.; Gnanasammandhan, M. K.; Zhang, Y. *Small* **2010**, *6*, 2781−2795.
(5) Wang, F.; Liu, X. *Chem. Soc. Rev.* **2009**, *38*, 976−989.

(6) Wu, S.; Han, G.; Milliron, D. J.; Aloni, S.; Altoe, V.; Talapin, D. V.; Cohen, B. E.; Schuck, P. J. *Proc. Natl. Acad. Sci. U.S.A.* **2009**, *106*, 10917−10921.
(7) Cheng, L.; Yang, K.; Li, Y.; Chen, J.; Wang, C.; Shao, M.; Lee, S. T.; Liu, Z. *Angew. Chem., Int. Ed.* **2011**, *123*, 7523−7528.
(8) Yang, J.; Zhang, C.; Peng, C.; Li, C.; Wang, L.; Chai, R.; Lin, J. *Chem.—Eur. J.* **2009**, *15*, 4649−4655.
(9) Li, Z.; Zhang, Y.; Jiang, S. *Adv. Mater.* **2008**, *20*, 4765−4769.
(10) Wang, C.; Cheng, L.; Liu, Z. *Biomaterials* **2011**, *32*, 1110−1120.
(11) Liu, K.; Liu, X.; Zeng, Q.; Zhang, Y.; Tu, L.; Liu, T.; Kong, X.; Wang, Y.; Cao, F.; Lambrechts, S. A. *ACS Nano* **2012**, *6*, 4054−4062.
(12) Yang, Y.; Velmurugan, B.; Liu, X.; Xing, B. *Small* **2013**, *9*, 2937−2944.
(13) Xiao, Q.; Bu, W.; Ren, Q.; Zhang, S.; Xing, H.; Chen, F.; Li, M.; Zheng, X.; Hua, Y.; Zhou, L. *Biomaterials* **2012**, *33*, 7530−7539.
(14) Castano, A. P.; Mroz, P.; Hamblin, M. R. *Nat. Rev. Cancer* **2006**, *6*, 535−545.
(15) Wang, F.; Banerjee, D.; Liu, Y.; Chen, X.; Liu, X. *Analyst* **2010**, *135*, 1839−1854.
(16) Zhou, J.; Liu, Z.; Li, F. *Chem. Soc. Rev.* **2012**, *41*, 1323−1349.
(17) Chatterjee, D. K.; Rufaihah, A. J.; Zhang, Y. *Biomaterials* **2008**, *29*, 937−943.
(18) Yang, Y.; Shao, Q.; Deng, R.; Wang, C.; Teng, X.; Cheng, K.; Cheng, Z.; Huang, L.; Liu, Z.; Liu, X. *Angew. Chem., Int. Ed.* **2012**, *51*, 3125−3129.
(19) Zhou, J.; Sun, Y.; Du, X.; Xiong, L.; Hu, H.; Li, F. *Biomaterials* **2010**, *31*, 3287−3295.
(20) Xing, H.; Bu, W.; Zhang, S.; Zheng, X.; Li, M.; Chen, F.; He, Q.; Zhou, L.; Peng, W.; Hua, Y. *Biomaterials* **2012**, *33*, 1079−1089.
(21) Kumar, R.; Nyk, M.; Ohulchanskyy, T. Y.; Flask, C. A.; Prasad, P. N. *Adv. Funct. Mater.* **2009**, *19*, 853−859.
(22) Nyk, M.; Kumar, R.; Ohulchanskyy, T. Y.; Bergey, E. J.; Prasad, P. N. *Nano Lett.* **2008**, *8*, 3834−3838.
(23) Xing, H.; Zheng, X.; Ren, Q.; Bu, W.; Ge, W.; Xiao, Q.; Zhang, S.; Wei, C.; Qu, H.; Wang, Z. *Sci. Rep.* **2013**, *33*, 1079−1089.
(24) Xiong, L.; Yang, T.; Yang, Y.; Xu, C.; Li, F. *Biomaterials* **2010**, *31*, 7078−7085.
(25) Mader, H. S.; Kele, P.; Saleh, S. M.; Wolfbeis, O. S. *Curr. Opin. Chem. Biol.* **2010**, *14*, 582−596.
(26) Wang, C.; Cheng, L.; Liu, Y.; Wang, X.; Ma, X.; Deng, Z.; Li, Y.; Liu, Z. *Adv. Funct. Mater.* **2013**, *23*, 3077−3086.
(27) Liu, J.; Bu, W.; Pan, L.; Shi, J. *Angew. Chem., Int. Ed.* **2013**, *52*, 4375−4379.
(28) Idris, N. M.; Gnanasammandhan, M. K.; Zhang, J.; Ho, P. C.; Mahendran, R.; Zhang, Y. *Nat. Med.* **2012**, *18*, 1580−1585.
(29) Chatterjee, D. K.; Yong, Z. *Nanomedicine* **2008**, *3*, 73−82.
(30) Qian, H. S.; Guo, H. C.; Ho, P. C. L.; Mahendran, R.; Zhang, Y. *Small* **2009**, *5*, 2285−2290.
(31) Prather, K. J.; Sagar, S.; Murphy, J.; Chartrain, M. *Enzyme Microb. Technol.* **2003**, *33*, 865−883.
(32) Ferreira, G. N.; Monteiro, G. A.; Prazeres, D. M.; Cabral, J. *Trends Biotechnol.* **2000**, *18*, 380−388.
(33) Mansouri, S.; Cuie, Y.; Winnik, F.; Shi, Q.; Lavigne, P.; Benderdour, M.; Beaumont, E.; Fernandes, J. C. *Biomaterials* **2006**, *27*, 2060−2065.
(34) Tan, W. B.; Jiang, S.; Zhang, Y. *Biomaterials* **2007**, *28*, 1565−1571.
(35) Pankhurst, Q. A.; Connolly, J.; Jones, S.; Dobson, J. *J. Phys. D: Appl. Phys.* **2003**, *36*, 167.
(36) Ito, A.; Shinkai, M.; Honda, H.; Kobayashi, T. *Cancer Gene Ther.* **2001**, *8*, 649.
(37) Derfus, A. M.; Chen, A. A.; Min, D.-H.; Ruoslahti, E.; Bhatia, S. N. *Bioconjug. Chem.* **2007**, *18*, 1391−1396.
(38) Yezhelyev, M. V.; Qi, L.; O'Regan, R. M.; Nie, S.; Gao, X. *J. Am. Chem. Soc.* **2008**, *130*, 9006−9012.
(39) Boisselier, E.; Astruc, D. *Chem. Soc. Rev.* **2009**, *38*, 1759−1782.
(40) Han, G.; You, C. C.; Kim, B. j.; Turingan, R. S.; Forbes, N. S.; Martin, C. T.; Rotello, V. M. *Angew. Chem., Int. Ed.* **2006**, *118*, 3237−3241.
(41) Jayakumar, M. K. G.; Idris, N. M.; Zhang, Y. *Proc. Natl. Acad. Sci. U.S.A.* **2012**, *109*, 8483−8488.
(42) Yang, Y.; Liu, F.; Liu, X.; Xing, B. *Nanoscale* **2013**, *5*, 231−238.
(43) Feng, L.; Zhang, S.; Liu, Z. *Nanoscale* **2011**, *3*, 1252−1257.
(44) Johnson, N. J.; Oakden, W.; Stanisz, G. J.; Scott Prosser, R.; van Veggel, F. C. *Chem. Mater.* **2011**, *23*, 3714−3722.
(45) Ryu, J.; Park, H.-Y.; Kim, K.; Kim, H.; Yoo, J. H.; Kang, M.; Im, K.; Grailhe, R.; Song, R. *J. Phys. Chem. C* **2010**, *114*, 21077−21082.
(46) He, M.; Huang, P.; Zhang, C.; Hu, H.; Bao, C.; Gao, G.; He, R.; Cui, D. *Adv. Funct. Mater.* **2011**, *21*, 4470−4477.
(47) Wang, F.; Han, Y.; Lim, C. S.; Lu, Y.; Wang, J.; Xu, J.; Chen, H.; Zhang, C.; Hong, M.; Liu, X. *Nature* **2010**, *463*, 1061−1065.
(48) Zhou, M.; Nakatani, E.; Gronenberg, L. S.; Tokimoto, T.; Wirth, M. J.; Hruby, V. J.; Roberts, A.; Lynch, R. M.; Ghosh, I. *Bioconjug. Chem.* **2007**, *18*, 323−332.
(49) Zhu, J.; Tang, A.; Law, L. P.; Feng, M.; Ho, K. M.; Lee, D. K.; Harris, F. W.; Li, P. *Bioconjug. Chem.* **2005**, *16*, 139−146.
(50) Tian, H.; Xiong, W.; Wei, J.; Wang, Y.; Chen, X.; Jing, X.; Zhu, Q. *Biomaterials* **2007**, *28*, 2899−2907.
(51) Feng, L.; Yang, X.; Shi, X.; Tan, X.; Peng, R.; Wang, J.; Liu, Z. *Small* **2013**, *9*, 1989−1997.
(52) Patnaik, S.; Aggarwal, A.; Nimesh, S.; Goel, A.; Ganguli, M.; Saini, N.; Singh, Y.; Gupta, K. *J. Controlled Release* **2006**, *114*, 398−409.
(53) Tiyaboonchai, W.; Woiszwillo, J.; Middaugh, C. R. *Eur. J. Pharm. Sci.* **2003**, *19*, 191−202.
(54) Durocher, Y.; Perret, S.; Kamen, A. *Nucleic Acids Res.* **2002**, *30*, 9.
(55) Kawakami, S.; Sato, A.; Nishikawa, M.; Yamashita, F.; Hashida, M. *Gene Ther.* **2000**, *7*, 292.
(56) Kakuta, K.; Orino, K.; Yamamoto, S.; Watanabe, K. *Comp. Biochem. Physiol., Part A: Mol. Integr. Physiol.* **1997**, *118*, 165−169.
(57) Huang, R.-Q.; Qu, Y.-H.; Ke, W.-L.; Zhu, J.-H.; Pei, Y.-Y.; Jiang, C. *FASEB J.* **2007**, *21*, 1117−1125.
(58) Yang, P.-H.; Sun, X.; Chiu, J.-F.; Sun, H.; He, Q.-Y. *Bioconjug. Chem.* **2005**, *16*, 494−496.
(59) Xu, L.; Pirollo, K. F.; Chang, E. H. *Hum. Gene Ther.* **1997**, *8*, 467−475.
(60) Cheng, P.-W. *Hum. Gene Ther.* **1996**, *7*, 275−282.
(61) Yang, A.; Liu, W.; Li, Z.; Jiang, L.; Xu, H.; Yang, X. *J. Nanosci. Nanotechnol.* **2010**, *10*, 622−628.
(62) Lesniak, A.; Campbell, A.; Monopoli, M. P.; Lynch, I.; Salvati, A.; Dawson, K. A. *Biomaterials* **2010**, *31*, 9511−9518.